

Phenotypic Adaptations in *Pasteuria* spp. Nematode Parasites

AURELIO CIANCIO¹

Abstract: The endospore and central core diameters of 69 isolates of *Pasteuria* spp. showed a relationship with the body wall thickness of their corresponding host nematodes. A relationship was also observed when cuticle and hypodermis layer data were derived from transmission electron microscopy micrographs. Principal component analysis and hierarchical cluster analysis based on endospore and central core diameters and host nematode body wall thickness delineated six distinct groups. Five groups included nematode species of distinct taxa. Endospore morphometric diversity appears to be the result of an evolutionary adaptation that occurred during host nematode speciation related to the forces acting on adhering endospores and/or to the host cuticle penetration phase. On this basis, the validity of endospore morphometrics and host taxonomy as significant parameters in discriminating *Pasteuria* species is questioned.

Key words: biological control, endospore adaptation, endospore adhesion, endospore diversity, endospore morphology, nematode parasite, *Pasteuria* spp.

Pasteuria penetrans (Actinomycetes) and related forms are obligate pathogens of nematodes with a potential for biological control of several plant-parasitic nematodes (17–20). Their life-cycle occurs entirely within the host body. The infective process is highly specific and occurs in soil, where the endospores, released from decaying hosts, adhere to the cuticle of passing nematodes. Adhesion is related to the number and integrity of the fibers surrounding the central endospore core that bind to the host cuticle (13). Germination can be observed after adhesion as a germ tube penetrates the cuticle. After germination, a dichotomously branching thallus develops within the host. Sporulation usually occurs when the host has been almost completely invaded by the vegetative thalli. At this stage, the thalli develop quartets, doublets, and finally single enlarged cells, each producing an endospore (8–10, 17,18).

Pasteuria spp. are widespread in different soil habitats and environments and have been observed on nematodes belonging to widely distinct taxa, including plant-

parasitic, predatory, and free-living or microbivorous species (4,7,12,17,24).

The infective endospores of the nematode-parasitic *Pasteuria* exhibit a wide range of morphometric and phenotypic diversity. Total endospore diameters vary from 2.2–2.7 μm for *P. thornei* that parasitizes *Pratylenchus brachyurus* to 6.5–8.0 μm for the *Pasteuria* that parasitize *Xiphinema* spp. and other Dorylaimida (4,23). Morphometric differences were also observed within different isolates of *P. penetrans* that parasitize *Meloidogyne* spp. Endospores of different sizes adhered to distinct host species with optimal attachment rates occurring at a given size. The passage through different host biotypes influenced the frequencies of endospores with higher or smaller diameters. When a single endospore size category was used to infect *M. incognita*, the endospores maintained similar size frequencies in the first generation (15).

Data from Sayre and Starr (17) concerning different host-*Pasteuria* associations show a positive linear correlation among endospore diameter and host minimum and maximum body lengths ($P < 0.001$). Morphometric diversity is considered to be related to host specificity, although little information is known about the mechanisms of parasitic adaptation or factors responsible for such diversity (3,4,18).

Phenotypic and morphometric differ-

Received for publication 3 June 1994.

¹ Istituto di Nematologia Agraria Applicata ai Vegetali, Consiglio Nazionale delle Ricerche, Via Amendola 165-A, 70126 Bari, Italy.

The author thanks R. Mankau and N. Vovlas for providing some nematode specimens and M. T. Melillo for assistance with TEM.

ences were used to separate new *Pasteuria* species, and *P. penetrans sensu stricto* was confined to the forms parasitic in root-knot nematodes (19,20,23). The main taxonomic criteria used for *Pasteuria* species description were endospore morphometrics and host. A multivariate analysis of a group of 65 *Pasteuria* forms from nematodes belonging to widely separated taxa did not show common clustering relationships between endospore dimensions and host taxonomic status (4). Other *P. penetrans* isolates from root-knot nematodes and cyst (*Heterodera* spp.) nematodes showed differences in their life cycles, sporulating in juveniles or adult nematodes (6,7,25).

The taxonomic relationships within *Pasteuria* are still poorly understood because cultures and/or pathotypes are not readily available for biochemical and genetic investigations. The morphometric diversity among several *Pasteuria* isolates was analyzed and the possible evolutionary implications of such diversity investigated. The mechanics of the endospore adhesion process and the properties and involvement of the host nematode cuticle are also discussed.

MATERIALS AND METHODS

Endospore and central core diameters were measured from *Pasteuria* spp. found adhering to or within nematode specimens from 65 species and deposited in different nematode collections (4). Other *Pasteuria*-nematode associations considered were: *P. penetrans* adhering to juveniles of *Meloidogyne incognita* and a *P. penetrans* form parasitic in *Helicotylenchus lobus*, originating from the University of California, Riverside; *Pasteuria* sp. parasitic in *Cephalobus* sp., collected by R. Mankau at Big Pine, California; and a *Pasteuria* sp., parasitic in juveniles of *Heterodera goettingiana*, originating from Faiano, Italy. The *Pasteuria* and nematode number designations are listed in Table 1.

The nematodes were extracted from soil by sieving, fixed in 2.5% formalin, dehy-

drated to glycerol, and subsequently mounted on glass slides for examination and measurements (22). The mean thickness of the cuticle, hypodermis, and somatic muscle layers (CHYSM) and the mean body diameters were measured on the same nematode specimens from which the endospore morphometric data were obtained. Measurements were taken using a Leitz Orthoplan light microscope and an oil immersion objective at $\times 2500$. Eight replicated measurements were taken along the nematodes from the dorsal and ventral regions, excluding the cephalic and tail regions.

The estimated basal area of endospore adhesion was calculated as: $BSA = \pi [(0.5 \times D_s)^2 + (0.5 \times D_c)^2]$, where D_s = mean endospore diameter and D_c = mean central core diameter.

Curve fitting was performed with continuous data trends using a quadratic polynomial equation of the type: $y = b_0 + b_1x + b_2x^2$. Quadratic fit and other calculations on nematode cuticle deformations were performed using the matrix operations provided by the program MathCad (MathSoft Inc., Cambridge, MA).

Multivariate analysis was performed using the endospore (SPO) and central core (COR) diameters and the CHYSM from each nematode-*Pasteuria* association, which was considered as a single statistical observation. Principal component analysis (PCA) and hierarchical cluster analysis (HCA) were performed using SAS programs (16). The detection of factors present in the original data matrix was determined by PCA through the calculation of new variables (principal components) that summarize the information dispersed in the original variables. The eigenvalues and the eigenvectors produced by PCA are the contribution of each component to the original variance and their correlation coefficients with the original variables, respectively. The correlation matrix of endospore and central core diameters and CHYSM was used for PCA. The average linkage method and the three resulting principal components were used for HCA.

TABLE 1. Host nematode species with *Pasteuria* spp. forms and number designations used for principal component and hierarchical cluster analysis.

Number	Host nematode species	Number	Host nematode species	Number	Host nematode species
1	<i>Acrobeloides</i> sp.	27	<i>Helicotylenchus vulgaris</i>	53	<i>Xiphinema basiri</i>
43	<i>Aphasmatylenchus nigeriensis</i>	62	<i>Heterodera fici</i>	38	<i>Xiphinema bergeri</i>
3	<i>Aphelenchoides rutgersi</i>	68	<i>Heterodera goettingiana</i>	63	<i>Xiphinema brasiliense</i>
58	<i>Axonchium valvulatum</i>	65	<i>Hoplotylus silvaticus</i>	39	<i>Xiphinema brevicolle</i>
4	<i>Boleodorus tylacthus</i>	12	<i>Longidorella parva</i>	48	<i>Xiphinema diversicaudatum</i>
69	<i>Cephalobus</i> sp.	7	<i>Longidorella</i> sp.	45	<i>Xiphinema ebriense</i>
2	<i>Coslenchus turkeyensis</i>	47	<i>Longidorus attenuatus</i>	35	<i>Xiphinema elongatum</i> (Philippines)
10	<i>Coslenchus costatus</i>	49	<i>Longidorus euonymus</i>	37	<i>Xiphinema elongatum</i> (Sri Lanka)
13	<i>Cylindrolaimus communis</i>	44	<i>Longidorus laevicapitatus</i> (Ethiopia)	51	<i>Xiphinema ifacolum</i>
6	<i>Discocriconemella mauritiensis</i>	42	<i>Longidorus laevicapitatus</i> (Liberia)	56	<i>Xiphinema ingens</i>
41	<i>Discolaimus major</i>	57	<i>Longidorus</i> sp.	34	<i>Xiphinema insigne</i>
24	<i>Dorylaimoides mitis</i>	67	<i>Meloidogyne incognita</i>	33	<i>Xiphinema longicaudatum</i>
64	<i>Eudorylaimus</i> sp.	19	<i>Merlinius brevidens</i>	22	<i>Xiphinema pachtaicum</i> (Italy)
11	<i>Helicotylenchus californicus</i>	8	<i>Merlinius</i> sp.	28	<i>Xiphinema pachtaicum</i> (Hungary)
16	<i>Helicotylenchus crenacauda</i>	23	<i>Opisthodorylaimus sylphoides</i>	52	<i>Xiphinema radiculicola</i>
17	<i>Helicotylenchus digonicus</i> (Algeria)†	55	<i>Paralongidorus citri</i>	46	<i>Xiphinema rotundatum</i>
18	<i>Helicotylenchus digonicus</i> (Malta)	15	<i>Paratrophurus anomalus</i>	32	<i>Xiphinema setariae</i> (Ethiopia)
20	<i>Helicotylenchus dihystrera</i>	9	<i>Pratylenchus neglectus</i>	36	<i>Xiphinema setariae</i> (Sri Lanka)
66	<i>Helicotylenchus lobus</i>	60	<i>Rotylenchus capensis</i>	25	<i>Xiphinema</i> sp. (Liberia)
61	<i>Helicotylenchus pseudorobustus</i> (Algeria)	50	<i>Rotylenchus laurentinus</i>	31	<i>Xiphinema</i> sp. (Somalia)
14	<i>Helicotylenchus pseudorobustus</i> (Greece)	40	<i>Scutellonema clathrycaudatum</i>	26	<i>Xiphinema</i> sp.
59	<i>Helicotylenchus pseudorobustus</i> (Italy)	5	<i>Tylenchulus semipenetrans</i>	54	<i>Xiphinema turcicum</i>
21	<i>Helicotylenchus pseudorobustus</i> (Peru)	30	<i>Xiphinema americanum</i>	29	<i>Xiphinema vuittenezi</i>

† Nematodes from the same species are distinguished in parentheses by their geographic origin.

For transmission electron microscopy (TEM), specimens of *H. lobus* with *P. penetrans* endospores within the body were fixed in 3% glutaraldehyde in phosphate buffer (0.05 M, pH 6.8), postfixed in an OsO_4 aqueous solution, dehydrated in a hexylene glycol series from 10% to 100%, and infiltrated with Spurr's medium. Sections 60–90 nm thick were cut using an LKB ultramicrotome III, stained with uranyl acetate and lead citrate, and examined with a Philips 400T Transmission Electron Microscope at 80 kV. Juvenile stages of *Heterodera fici* encumbered with endospores were prepared and examined as described (1). Other measurements of *Pasteuria* endospores and host cuticle (CUT), cuticle and hypodermis (CHY), and CHYSM were obtained from published data and TEM micrographs (7,18,23,25).

RESULTS

A linear relationship was observed between the *Pasteuria* endospore and central core diameters and the CHYSM value of the corresponding host nematodes, when nematodes were examined by light microscopy (Fig. 1B,C; Table 2). The endospore and core diameters from TEM measurements were also positively correlated with the depths of the host cuticle and the cuticle-hypodermis layers (Fig. 1A,D–E; Table 3). Quadratic curve fitting showed for both variables a less pronounced linkage at CHYSM higher values (Figs. 2,3). A positive correlation occurred between the endospore diameters and host CHYSM value when the analysis was limited to species of the genus *Xiphinema* ($r = 0.60$, $P < 0.01$). Significant positive correlations between endospore morphometrics and CHYSM were also found when the analysis was limited to species from the orders Tylenchida and Dorylaimida (Table 2). BSA was positively correlated with CHYSM ($r = 0.78$, $P < 0.001$), and the relationship between the two variables appeared effective even at the higher CHYSM values (Fig. 4). The core-to-endospore ratio showed an inverse

correlation with CHYSM ($r = -0.55$, $P < 0.001$). Endospore and central core diameters from a set of 57 available specimens were correlated with the average nematode body diameter ($r = 0.71$, $P < 0.001$, and $r = 0.35$, $P < 0.01$, respectively).

The variance associated with the first and second principal components was 95.7% of total (Table 4). Six distinct groups were identified by HCA on the first and second component axes (Fig. 5). The first principal component showed positive correlations ($P < 0.001$) with all the variables used (Table 5). Along this axis, the observations were distributed with increasing endospore morphometrics and host CHYSM. The second principal component, accounting for 17.33% of total variance, showed a positive correlation with the core diameter and a significant inverse correlation with CHYSM ($P < 0.001$). Along this axis, it was possible to distinguish clusters with mean CHYSM per endospore core ratios higher than 2.5 (groups IV and VI) from groups with ratios lower than 1.8 (groups I, II, III, V) (Table 6). This axis was interpreted as a factor accounting for some divergence in host-parasite coevolutionary trends, separating two clusters composed exclusively of large host species from the order Dorylaimida (Figs. 5,6).

The cluster species composition varied among different host families and orders. Five groups included forms and host species of the same genera, as well as species from other distinct taxa. Groups I and III included *Pasteuria* forms associated with plant-parasitic and free-living hosts from different orders. Groups II and V included forms and nematodes belonging only to the orders Dorylaimida and Tylenchida. Group IV was composed of forms associated with plant-parasitic and predacious species of the order Dorylaimida. Group VI included only three *Xiphinema-Pasteuria* associations (Table 6; Fig. 6).

When the portion of cuticle involved in endospore adhesion was considered schematically as a transverse circular sector and

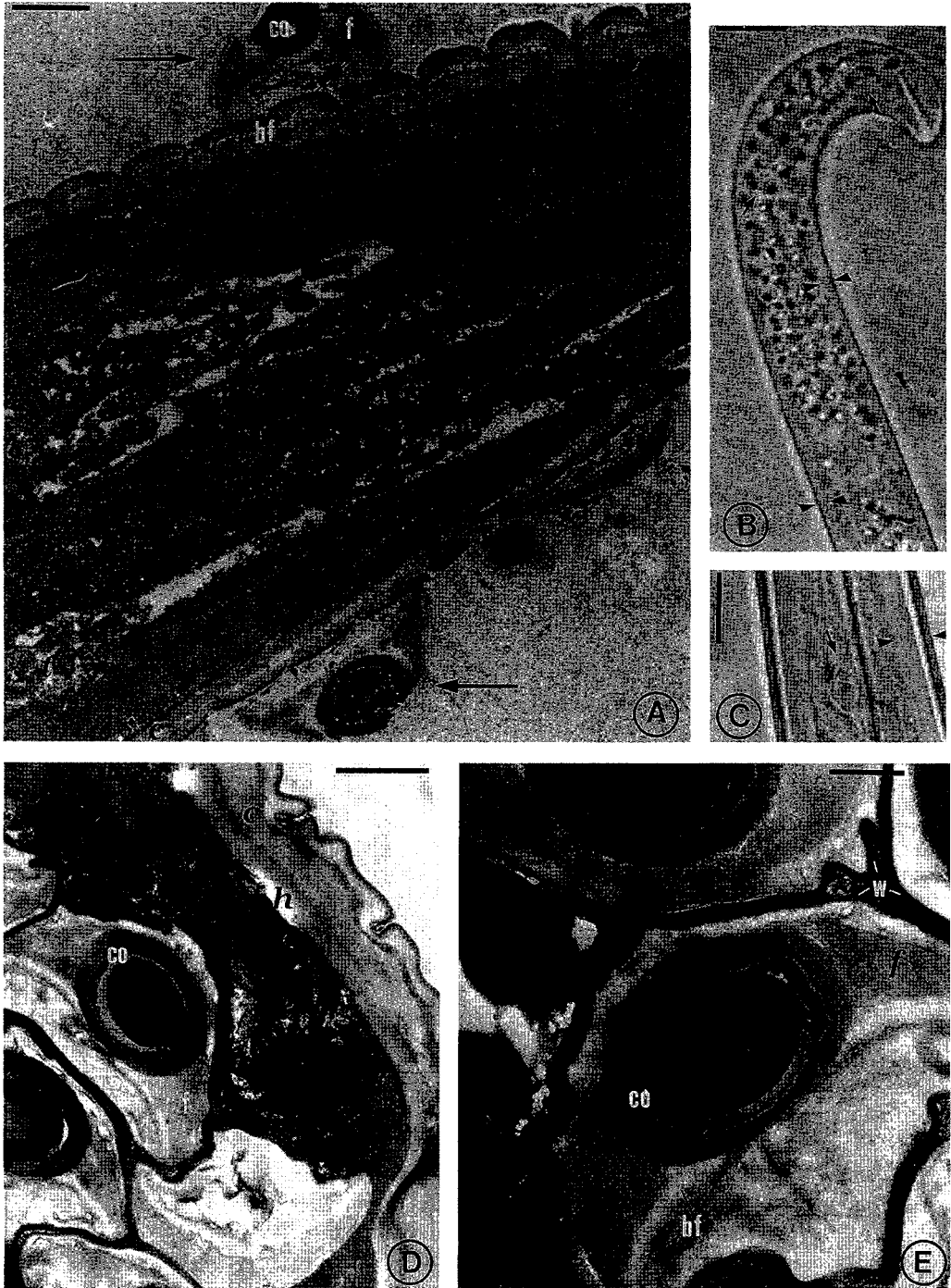


FIG. 1. Transmission electron microscopy (TEM) and light microscopy images of *Pasteuria* spp. parasitic in plant-parasitic nematodes. A) TEM longitudinal section of a juvenile *Heterodera fici* with endospores adhering to the cuticle (arrows) and vegetative thalli (t). B) Small endospore *Pasteuria* form within a living juvenile *Tylenchulus semipenetrans*. C) Large endospore *Pasteuria* form within *Longidorus attenuatus*. D–E) TEM micrographs of *Pasteuria penetrans* resting endospores from parasitized *Helicotylenchus lobus*. bf = basal parasporal fibers, c = cuticle, co = central endospore core, f = parasporal fibers, h = hypodermis, m = somatic muscles, t = vegetative thalli, w = sporangial wall. Arrows (B,C) show the measured layers of the body wall. Scale bars: A = 1.5 μm ; B,C = 10 μm ; D = 1 μm ; E = 0.5 μm .

TABLE 2. Pearson's correlation coefficients between the endospore (SPO) and central core diameters (COR) of *Pasteuria* spp. and the corresponding host cuticle, hypodermis and somatic muscle thickness (CHYSM). Data are from all grouped nematode species listed in Table 1 and two sets of observations from orders Tylenchida and Dorylaimida.†

	All nematode species		Tylenchida		Dorylaimida	
	SPO	COR	SPO	COR	SPO	COR
COR	0.74***		0.91***		0.90***	
CHYSM	0.79***	0.48***	0.85***	0.81***	0.58**	0.41*

† Data obtained using light microscopy measurements.

* $P < 0.05$; ** $P < 0.01$; *** $P < 0.001$.

the nematode body was represented as an elastic cylinder, simulated radial coaxial contractions due to elongation yielded linear changes in cuticle length ranging in the order of a few hundred nanometers. At a longitudinal increase corresponding to 5% of nematode length, the contraction due to elongation was $0.168 \mu\text{m}$ for a cuticle sector of $7 \mu\text{m}$ and $0.072 \mu\text{m}$ for a cuticle sector of $3 \mu\text{m}$.

When the forces acting on endospores adhering to the nematode cuticle were schematically represented as inclined vectors, it was possible to identify two normal components. The first component was perpendicular to the host cuticle and acted in the direction of the adhesive force. The effect of this force was the strengthening of endospore adherence to the cuticle. The second component was parallel to the host

cuticle. This component had a translational effect with respect to the endospore-cuticle normal axis and the cuticular area involved in adhesion (Fig. 7).

DISCUSSION

Nematodes rely on a hydrostatic skeleton for movement. Their motion is produced through a number of internal and external forces, which act on the cuticle, producing a sequence of alternated elongations and contractions (21,27). The nematode body structure can be schematically represented as an elastic cylinder whose locomotion depends on contractions that alter the body diameter as its volume remains constant (2).

TABLE 3. Pearson's correlation coefficients between the host body wall thickness measured from transmission electron microscopy (TEM) micrographs and the *Pasteuria* spp. endospore measurements. Host nematode species: *Belonolaimus longicaudatus*, *Hoplolaimus galeatus*, *Pratylenchus brachyurus*, *Meloidogyne incognita*, *Helicotylenchus lobus*, *Heterodera fici*, and *Heterodera goettingiana*.†

	SPO	COR	CHYSM	CHY
COR	0.97***			
CHYSM	0.72*	0.75*		
CHY	0.85**	0.86**	0.81*	
CUT	0.80*	0.81*	0.75*	0.87*

† SPO = mean endospore diameter; COR = mean central core diameter; CHYSM = cuticle, hypodermis and somatic muscle thickness; CHY = cuticle and hypodermis thickness; CUT = cuticle thickness. Body wall data are from TEM micrographs in citations 7,17,23, and 25 and from Fig. 1A,D. Endospore and central core data as reported by the authors or measured by light microscopy.

* $P < 0.05$; ** $P < 0.01$; *** $P < 0.001$.

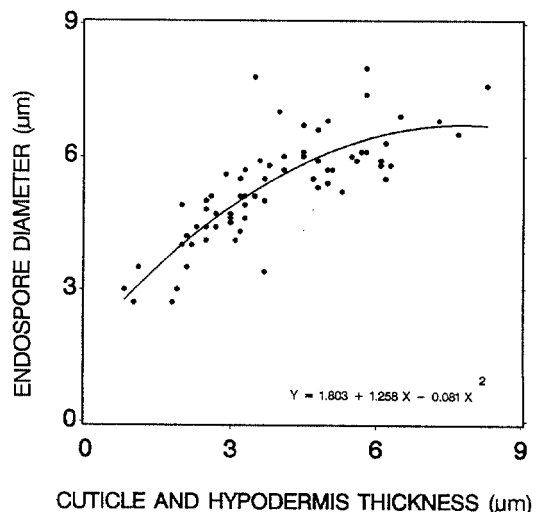


FIG. 2. Relationship between the thickness of the host nematode cuticle, hypodermis, and somatic muscle layers (CHYSM) from 69 nematode species as listed in Table 1 and the total endospore diameter of the associated *Pasteuria* forms.

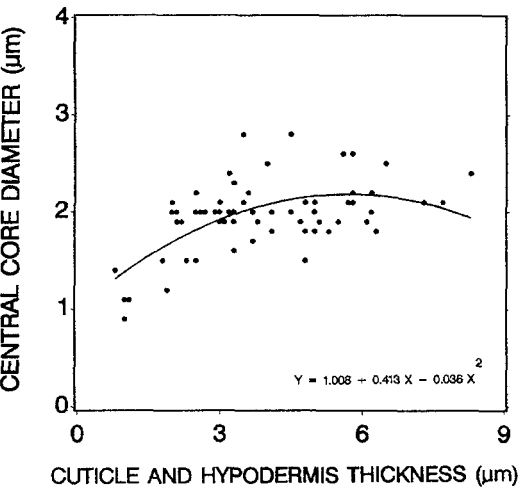


FIG. 3. Relationship between the thickness of the host nematode cuticle, hypodermis, and somatic muscle layers (CHYSM) from 69 nematode species as listed in Table 1 and the core diameter of the associated *Pasteuria* forms.

Transverse striations allow the nematode cuticle to withstand the alternated anisometric longitudinal extensions and compressions due to the combined effect of the longitudinal muscles and the turgor pressure system (2). Other local cuticle deformations are also produced by internal pro-

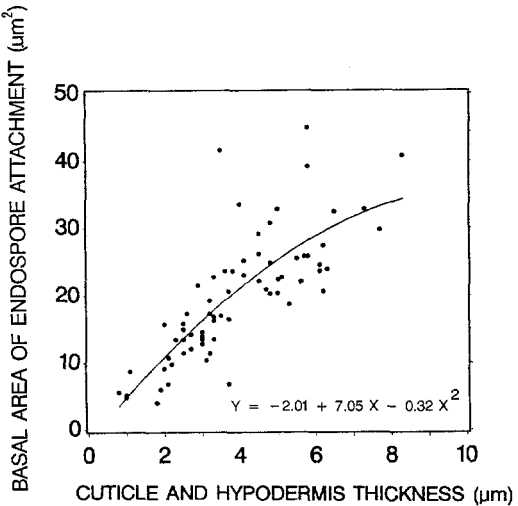


FIG. 4. Relationship between the thickness of the host nematode cuticle, hypodermis, and somatic muscle layers (CHYSM) from 69 nematode species as listed in Table 1 and the estimated endospore adhesion area of the associated *Pasteuria* forms.

TABLE 4. Eigenvalues of the correlation matrix used for principal component analysis of endospore diameters, central core diameters and cuticle, hypodermis and somatic muscle thickness and proportion and cumulative percentages of total variance explained by each principal component.

Principal component	Eigenvalue	Proportion	Cumulative
First	2.350	0.78	0.78
Second	0.520	0.17	0.95
Third	0.129	0.04	1.00

cesses, i.e., defecation or egg deposition (21).

All the internal forces produced by nematodes also act on the adhering *Pasteuria* endospores and interact with the external friction forces resulting from endospore contact with soil particles or from movement of endo- or semi-endoparasitic hosts through plant cells.

Along a nematode longitudinal axis, any cuticle elongation or contraction will tend to displace the endospore (or fibers) adhesion points inward or outward. The displacements that the endospore fibers ad-

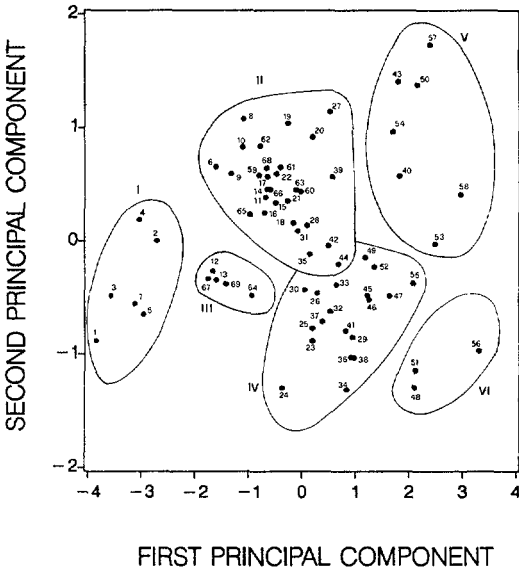


FIG. 5. Plot of the 69 host nematode-*Pasteuria* spp. associations on the first and second principal components factorial plan. Clusters derived from hierarchical cluster analysis dendrogram at 40% of total distance. See Table 1 for host nematode species numbers.

TABLE 5. Eigenvectors of the correlation matrix used for principal component analysis of endospore diameters (SPO), central core diameters (COR) and cuticle, hypodermis and somatic muscle thickness (CHYSM) from 69 *Pasteuria*-host nematode associations. Values are correlation coefficients of principal components with the original variables used.

Variables†	Principal components		
	First	Second	Third
SPO	0.62***	-0.04	-0.77***
COR	0.54***	0.74***	0.38**
CHYSM	0.56***	-0.66***	0.49***

† SPO = mean spore diameter; COR = mean central core diameter; CHYSM = cuticle, hypodermis and somatic muscle thickness.

* $P < 0.05$; ** $P < 0.01$; *** $P < 0.001$.

hering to the cuticle must adapt to (due to elongation or contraction) are, however, independent of body diameter, depending on the extent of longitudinal deformations.

Pasteuria spp. endospores show a common structural organization. Parasporal fibers surround the central core, and their distribution and function appear relatively uniform when viewed with TEM (5,7,18, 20). Some observed differences, however, were used as the basis to describe new species (20,23,25). However, the fibers allowing spore adhesion and the limited changes produced by host movements do

not appear sufficient to suggest an adaptive morphometric process determined only by the mechanical properties of the host cuticle (i.e., bending and flexibility). The cuticle deformations related to locomotion are small in scale, and an elastic endospore reaction can prevent detachment or displacement. This reaction involves the parasporal and adhesive fibers present on the peripheral and basal endospore areas. When adhering to the host, the basal and peripheral endospore fibers can display different insertion angles with the cuticle. Their movements allow the adhesion points to be displaced during host contractions without affecting adhesion and core location. An elastic response can also allow endospores to withstand other translational vectors similar to those resulting from friction forces.

Considering the relationship between endospore diameters, body length, and cuticle thickness, it seems possible that endospore morphometric diversity could represent an adaptive response to the strength of the forces discharged on the endospore, rather than to the degree of the elastic cuticle modifications.

The observed correlations also suggest the occurrence of a second selective pressure acting mainly on small- and medium-

TABLE 6. Mean and range values of endospore (SPO), central core (COR), and cuticle, hypodermis and somatic muscle thickness (CHYSM) and species composition of the groups identified by hierarchical cluster analysis.

Group	Species†	SPO††	COR††	CHYSM††
I	1 2 3 4 5 7	2.9 (2.7–3.0) a	1.2 (0.9–1.5) a	1.2 (0.8–1.9) a
II	6 8 9 10 17 11 14 15 16 18 19 20 21 22 27 28 31 35 39 42 44 59 60 61 62 63 65 66 68	4.9 (3.5–6.1) b	2.0 (1.9–2.4) bc	3.0 (2.0–4.5) b
III	12 13 64 69 67	4.2 (3.4–4.9) b	1.5 (1.5–1.7) d	2.8 (2.3–3.7) b
IV	23 24 25 26 29 30 32 33 34 33 37 38 41 45 46 47 49 52 55	5.9 (5.2–7.4) c	1.9 (1.8–2.2) b	5.3 (4.1–6.3) c
V	40 43 50 53 54 57 58	6.9 (5.9–8.0) d	2.6 (2.5–2.8) e	4.9 (3.5–6.5) c
VI	48 51 56	6.9 (6.5–7.6) d	2.2 (2.1–2.4) c	7.7 (7.3–8.3) d

† For species numbers, see Table 1.

†† Mean and range values in μm . Data in columns with the same letter do not differ significantly according to Duncan's multiple-range test ($P < 0.01$).

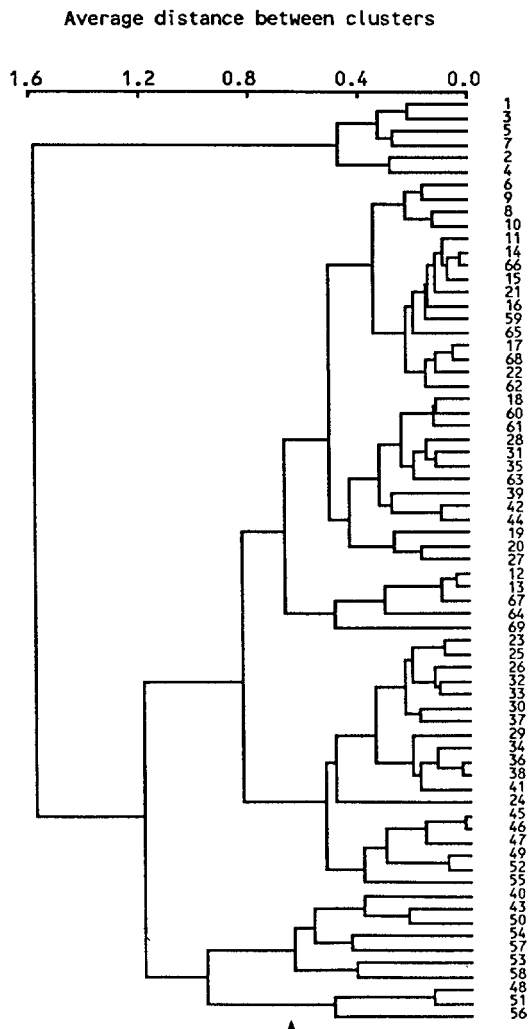


FIG. 6. Dendrogram produced by average linkage cluster analysis of the host nematodes and associated *Pasteuria* forms. Clusters disjoined at 40% of total distance (arrow). See Table 1 for numbers of host nematode species.

size endospore forms, and related to the adhesion-germination phase. The absence of vegetative growth of the germination peg inside the initially penetrated host cuticular layers could be a further selective barrier. Therefore, endospore size may result as a correlated response to selection, required to maintain the endospore firmly in place before germination occurs. Other morphological characters (i.e., fiber arrangements, core shape, core wall layers) may have evolved without direct relationship with host body size or as the result of genetic drifts.

A functional adaptation of endospore and core diameters to the host body wall is supported by the obligate parasitic behavior of the nematode-pathogenic *Pasteuria* forms and by their narrow host ranges (6,12). All the germinating endospores observed thus far (5,17,19,25) showed penetration but not dichotomous growth of the extruding peg within the cuticle and(or) the associated hypodermis layers. Although penetration is considered as proceeding through an enzymatic activity (11), developing vegetative thalli were almost always observed below the layers of host somatic muscles (4,19,25). Light microscopy observations never showed further lytic activities of *Pasteuria* vegetative microcolonies affecting the host cuticle after penetration (5,19,25,28). This particular behavior can be favorable for the parasite. During parasitism, the host nematode cuticle acts as a protective barrier and as a container for the parasite propagules until host decomposition. As a limited amount of energy appears available for growth during cuticle penetration, the germination pegs must rely on the energy sources stored inside the endospore core for development. Greater distances required to reach an energy or metabolic source available for vegetative development could require higher reserves stored in the core with corresponding increases in endospore dimensions. Larger cores also require a wider endospore and fiber organization to remain attached until germination because of host movements and acting friction forces.

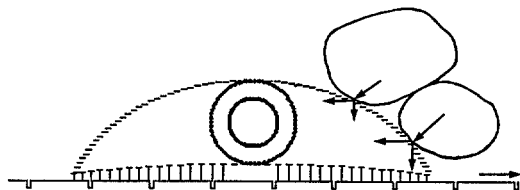


FIG. 7. A schematic drawing of the friction forces acting on a *Pasteuria* spore adhering to the cuticle of a host nematode moving through soil particles. Arrow shows movement direction.

The hypothesis of a *Pasteuria* metabolic preference for the inner pseudocoelomic host tissues is supported by the observation that parasitized nematodes filled with endospores were capable of movement, suggesting a limited destruction of their muscular system (4,5,26). In several parasitized specimens, the gonads, pharynx, and other sclerotized tissues or organs (i.e., spear, spiculae, vulvular lips) were not destroyed by the parasite's development (4,5,7,23,26). The correlations observed for TEM measurements showed that core and endospore dimensions were mainly related to the host cuticle and hypodermis and, to a lesser degree, to the depth of the somatic muscles. The decrease in the core-to-endospore ratio at increasing body wall thickness and the relatively uniform core dimensions for large *Pasteuria* forms show that somatic muscles, which have higher volume and length in Longidorid nematodes, had a minor effect on the observed relationships.

Convergent evolutionary trends or wide host ranges (12) could explain the absence of a direct relationship between endospore morphometrics and host taxonomic status, as revealed by PCA and HCA. Genetic drifts, peak shifts of alternative optima for core and endospore sizes (14), and wider host ranges (12) could also account for the morphometric diversity observed among forms from the same nematode genera (4) or for the different clustering affinities shown mainly by forms from dorylaim hosts.

Morphometric criteria are not sufficient to represent and explain the diversity of *Pasteuria* forms. This conclusion is supported by the clustering of the *P. penetrans* type isolate with forms from phylogenetically distant hosts. Further evidence is provided by forms from related nematode species (i.e., *Xiphinema pachtaicum* and *X. americanum*; *Rotylenchus laurentinus* and *R. capensis*), which clustered in distinct groups. A generic distinction was possible, however, among groups with small, medium, and large endospore size forms.

The lack of evidence for unique associ-

ations between host taxa and parasite morphometrics does not necessarily reduce the *Pasteuria* complex to a single nematode parasitic species (*P. penetrans*). It suggests, however, a revision of the taxonomic criteria proposed for this group of microorganisms. Different host-specific pathotypes may occur within one or more *Pasteuria* species. A hypothesis concerning the evolutionary trends in the genus *Pasteuria* will require more homogeneous characters based on gene sequences or metabolic requirements.

LITERATURE CITED

1. Abrantes, I. M. de O., and N. Vovlas. 1988. A note on parasitism of the phytonematodes *Meloidogyne* sp. and *Heterodera fici* by *Pasteuria penetrans*. Canadian Journal of Zoology 66:2852-2854.
2. Calcoen, J., and D. R. Roggen. 1973. The form of moving nematodes. Nematologica 19:408-410.
3. Ciancio, A. 1991. Relationship between spore dimensions and body cuticle thickness in *Pasteuria penetrans*-infected nematodes. Journal of Nematology 23:525 (Abstr.).
4. Ciancio, A., R. Bonsignore, N. Vovlas, and F. Lamberti. 1994. Host records and spore morphometrics of *Pasteuria penetrans* group parasites of nematodes. Journal of Invertebrate Pathology 63:260-267.
5. Ciancio, A., R. Mankau, and M. Mundo-Ocampo. 1992. Parasitism of *Helicotylenchus lobus* by *Pasteuria penetrans* in a naturally infested soil. Journal of Nematology 24:29-35.
6. Davis, K. G., C. A. Flynn, V. Laird, and B. K. Kerry. 1990. The life cycle, population dynamics, and host specificity of a parasite of *Heterodera avenae*, similar to *Pasteuria penetrans*. Revue de Nématologie 13:303-309.
7. Giblin-Davis, R. M., L. L. McDaniel, and F. G. Bilz. 1990. Isolates of the *Pasteuria penetrans* group from phytoparasitic nematodes in bermudagrass turf. Supplement to the Journal of Nematology 22:750-762.
8. Imbriani, J. L., and Mankau, R. 1977. Ultrastructure of the nematode pathogen, *Bacillus penetrans*. Journal of Invertebrate Pathology 30:337-347.
9. Mankau, R. 1975. *Bacillus penetrans* n. comb. causing a virulent disease of plant-parasitic nematodes. Journal of Invertebrate Pathology 26:333-339.
10. Mankau, R., and J. L. Imbriani. 1975. The life cycle of an endoparasite in some tylenchid nematodes. Nematologica 21:89-94.
11. Mankau, R., J. L. Imbriani, and A. H. Bell. 1976. SEM observations on nematode cuticle penetration by *Bacillus penetrans*. Journal of Nematology 8:179-181.
12. Oostendorp, M., D. W. Dickson, and D. J. Mitchell. 1990. Host range and ecology of isolates of

Pasteuria spp. from the Southeastern United States. *Journal of Nematology* 22:525–531.

13. Persidis, A., J. G. Lay, T. Manousis, A. H. Bishop, and D. J. Ellar. 1991. Characterization of potential adhesins of the bacterium *Pasteuria penetrans*, and of putative receptors on the cuticle of *Meloidogyne incognita*, a nematode host. *Journal of Cell Science* 100:613–622.

14. Price, T., M. Turelli, and M. Slatkin. 1993. Peak shifts produced by correlated responses to selection. *Evolution* 47:280–290.

15. Ratnasoma, H. A., and S. R. Gowen. 1991. Studies on the spore size of *Pasteuria penetrans* and its significance on the spore attachment process on *Meloidogyne* spp. *Afro-Asian Journal of Nematology* 1:51–56.

16. SAS Institute. 1985. SAS user's guide. Cary, NC: SAS Institute.

17. Sayre, R. M., and M. P. Starr. 1985. *Pasteuria penetrans* (ex Thorne, 1940) nom. rev., comb. n., sp. n., a mycelial and endospore-forming bacterium parasitic in plant-parasitic nematodes. *Proceedings of the Helminthological Society of Washington* 52:149–165.

18. Sayre, R. M., and W. P. Wergin. 1977. Bacterial parasite of a plant nematode: Morphology and ultrastructure. *Journal of Bacteriology* 129:1091–1101.

19. Sayre, R. M., M. P. Starr, A. Morgan Golden, W. P. Wergin, and B. Y. Endo. 1988. Comparison of *Pasteuria penetrans* from *Meloidogyne incognita* with a related mycelial and endospore-forming bacterial parasite from *Pratylenchus brachyurus*. *Proceedings of the Helminthological Society of Washington* 55:28–49.

20. Sayre, R. M., W. P. Wergin, J. M. Schmidt, and

M. P. Starr. 1991. *Pasteuria nishizawae* sp. nov., a mycelial and endospore-forming bacterium parasitic on cyst nematodes of genera *Heterodera* and *Globodera*. *Research in Microbiology* 142:551–564.

21. Seymour, M. K. 1973. Motion and the skeleton in small nematodes. *Nematologica* 19:43–48.

22. Southey, J. F., ed. 1970. Laboratory methods for work with plant and soil nematodes. Technical Bulletin No. 2. London: Her Majesty's Stationery Office.

23. Starr, M. P., and R. M. Sayre. 1988. *Pasteuria thornei* sp. nov. and *Pasteuria penetrans sensu stricto* emend., mycelial and endospore-forming bacteria parasitic, respectively, on plant parasitic nematodes of the genera *Pratylenchus* and *Meloidogyne*. *Annales de l'Institut Pasteur/Microbiologie*, 139:11–31.

24. Sturhan, D. 1988. New hosts and geographical records of nematode parasitic bacteria of the *Pasteuria penetrans* group. *Nematologica* 34:350–356.

25. Sturhan, D., R. Winkelheide, R. M. Sayre, and W. P. Wergin. 1994. Light and electron microscopical studies of the life cycle and developmental stages of a *Pasteuria* isolate parasitizing the pea cyst nematode, *Heterodera goettingiana*. *Applied and Fundamental Nematology* 17:29–42.

26. Vovlas, N., A. Ciancio, and E. Vlachopoulos. 1993. *Pasteuria penetrans* parasitizing *Helicotylenchus pseudorobustus* and *Rotylenchus capensis* in Greece. *Afro-Asian Journal of Nematology* 3:39–42.

27. Wharton, D. A. 1986. A functional biology of nematodes. Baltimore, MD: The Johns Hopkins University Press.

28. Williams, J. R. 1967. Observations on parasitic protozoa in plant-parasitic and free-living nematodes. *Nematologica* 13:336–342.